Acta Pharmaceutica Sinica B 2021;11(1):258–270

Chinese Pharmaceutical Association
Institute of Materia Medica, Chinese Academy of Medical Sciences

Acta Pharmaceutica Sinica B

www.elsevier.com/locate/apsb
www.sciencedirect.com

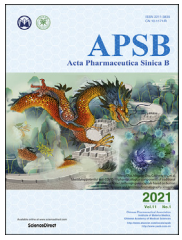

ORIGINAL ARTICLE

# A facile and universal method to achieve liposomal remote loading of non-ionizable drugs with outstanding safety profiles and therapeutic effect

**Shuang Zhou[a], Jinbo Li[a], Jiang Yu[a], Liyuan Yang[a], Xiao Kuang[a], Zhenjie Wang[a], Yingli Wang[a], Hongzhuo Liu[a], Guimei Lin[c], Zhonggui He[a], Dan Liu[b,*], Yongjun Wang[a,*]**

[a]*Wuya College of Innovation, Shenyang Pharmaceutical University, Shenyang 110016, China*
[b]*Key Laboratory of Structure-Based Drugs Design & Discovery of Ministry of Education, Shenyang Pharmaceutical University, Shenyang 110016, China*
[c]*School of Pharmaceutical Science, Shandong University, Jinan 250012, China*

Received 25 June 2020; received in revised form 3 August 2020; accepted 5 August 2020

**KEY WORDS**

Non-ionizable drugs;
Weak acid derivatives;
Remote loading liposome;
Cabazitaxel;
Safety;
Tolerated doses;
Cancer;

**Abstract** Liposomes have made remarkable achievements as drug delivery vehicles in the clinic. Liposomal products mostly benefited from remote drug loading techniques that succeeded in amphipathic and/or ionizable drugs, but seemed impracticable for nonionizable and poorly water-soluble therapeutic agents, thereby impeding extensive promising drugs to hitchhike liposomal vehicles for disease therapy. In this study, a series of weak acid drug derivatives were designed by a simplistic one step synthesis, which could be remotely loaded into liposomes by pH gradient method. Cabazitaxel (CTX) weak acid derivatives were selected to evaluate regarding its safety profiles, pharmacodynamics, and pharmacokinetics. CTX weak acid derivative liposomes were superior to Jevtana® in terms of safety profiles,

*Abbreviations:* $AUC_{0-t}$, area under the curve; Chol, cholesterol; CR, creatinine; CTX, cabazitaxel; DA, *trans*-2-butene-1,4-dicarboxylic acid; DA-CTX, cabazitaxel *trans*-2-butene-1,4-dicarboxylic acid derivate; DSPC, 1,2-dioctadecanoyl-*sn*-glycero-3-phophocholine; DSPE-PEG2000, 2-distearoyl-snglycero-3-phosphoethanolamine-*N*-[methyl(polyethylene glycol)-2000; EE, encapsulation efficiency; EPR, enhanced permeability and retention; GA, glutaric anhydride; GA-CTX, cabazitaxel glutaric acid derivate; lipo DA-CTX, DA-CTX liposome; lipo GA-CTX, GA-CTX liposome; lipo SA-CTX, SA-CTX liposome; mCRPCa, metastatic castration-resistant prostate cancer; MED, minimum effective dose; MPS, mononuclear phagocyte system; MTD, maximum tolerated dose; PCa, prostate cancer; PSA, prostate-specific antigen; SA, succinic anhydride; SA-CTX, cabazitaxel succinic acid derivate; TI, therapeutic index.

*Corresponding authors.
E-mail addresses: sammyld@163.com (Dan Liu), wangyongjun@syphu.edu.cn (Yongjun Wang).

Peer review under responsibility of Chinese Pharmaceutical Association and Institute of Materia Medica, Chinese Academy of Medical Sciences.

https://doi.org/10.1016/j.apsb.2020.08.001

Lung metastasis

including systemic toxicity, hematological toxicity, and potential central nerve toxicity. Specifically, it was demonstrated that liposomes had capacity to weaken potential toxicity of CTX on cortex and hippocampus neurons. Significant advantages of CTX weak acid derivative-loaded liposomes were achieved in prostate cancer and metastatic cancer therapy resulting from higher safety and elevated tolerated doses.



## 1. Introduction

"Druggable compounds" require chemical entities with features of water-solubility and bioavailability[1]. However, many chemical structures discovered and synthesized were barely soluble, had low bioavailability, and caused significant system toxicity[2]. Most antineoplastic chemical drugs have low performance regarding water-solubility, bioavailability, and safe profiles. Although a prodrug strategy has been developed to improve physicochemical properties, which potentially augmented stability, bioavailability and lowered toxicity, the bioactivity declined as well[1,2]. As a result, extensive studies currently focused on the exploitation of nanotechnology for chemotherapy drug delivery, trying to improve the therapeutic index and augmenting therapeutic efficacy[3,4]. It is believed that nanoparticles can selectively enhance the concentration of the active ingredient in tumors because of the enhanced permeability and retention (EPR) effect, which results from a leaky and highly abnormal vascular system of the tumor, while enhancing retention results from the disordered lymphatic system, which is characteristic of malignant tumors[5,6]. Among various nanoparticles, liposomes are recognized as one of the most successful and promising commercial nano drug delivery systems which have demonstrated nanoparticles with safer profiles when compared to many conventional drugs[7−11]. The liposome resembles a biological cell membrane regarding structure and composition and has been considered as a promising candidate for the improvement of drug delivery systems. The biocompatible and biodegradable liposomes can encapsulate both hydrophilic and hydrophobic drugs, making them attractive vehicles in the field of drug delivery[12]. Many liposomal products are available for application in clinical therapy, including doxorubicin hydrochloride liposome (Doxil®), daunorubicin liposome (DaunoXome®), irinotecan liposome (Onivyde®), vincristine sulfate (Marqibo®), daunorubicin, and cytarabine co-encapsulated liposomes (Vyxeos®)[7]. Some of the side effects of conventional drugs could be overcame when formulated into liposomes, thus enhancing the therapeutic index of various drugs, and having positive impacts on patients' health. Sate of the art of liposome manufacture technology ensures industrialization feasibility[13,14]. Such great achievements of liposomes have inspired researchers to investigate drug liposomes formulations extensively and deeply.

Theoretically, either hydrophobic or hydrophilic molecules could be loaded into liposomes in the lipid bilayer or internal aqueous environment[7]. Sparingly water-soluble drugs are generally intercalated into the liposome bilayer, namely passive loading, with a limited capacity and poor drug retention. It renders the drugs prone to the release and dissociation after administration, resulting in little improvements in safety and therapeutic efficacy[15]. The invention of "remote" drug loading methods of liposomes drives more commercial products forward to clinical applications due to the superiority of remote drug loading methods that presented high drug-to-lipid, encapsulation efficiency, and stable retainment of drugs[16]. An ammonium ion gradient or low pH citrate buffer has successfully been utilized for the remote loading of amphipathic weak basic drugs, such as doxorubicin hydrochloride and vincristine sulfate, while an acetate gradient is appropriate for the remote loading of amphipathic weak acidic drugs[17]. The first liposomal product Doxil®, a specific formulation of doxorubicin enclosed in unilamellar liposomal vesicles, was developed to treat various types of cancers ranging from metastatic ovarian cancer to AIDS-related Kaposi's Sarcoma. Cardiac toxicity was remarkably reduced, resulting in spectacular success when Doxil® was available[18]. The liposomal products mentioned above are all prepared by a remote loading method. Although many advantages were occupied by liposomes, physicochemical properties of surplus drugs of interest, exhibiting either bad aqueous solubility or membrane permeability, were not suitable for remote loading. The transition metal ion gradient method provided an alternative approach for drugs, which contained metal ions binding sites[19]. Remote drug loading techniques were not considered as a universal and common methodology for drugs that were highly hydrophobic or lacked an ionizable group, such as taxanes. Consequently, many approaches have been devised to circumvent this predicament. For ionizable poorly soluble drugs, a solvent-assisted active loading technology was developed to use miscible solvent assist drugs to go cross the lipid membrane, which was easier than the preceding way[20]. This facile approach was powerful in sweeping away the obstacle of poorly soluble drugs; however, it was still based on an existing remote loading method, and could not be realized for drugs that were non-ionizable and had unequipped metal ion binding sites or functional groups. Functional cyclodextrin was chemically modified to ferry drugs into liposomes[21]. This strategy required that drugs have a higher affinity with cyclodextrin compared to cholesterol, and required an additional procedure with a long process preparation. Chemical modification of the drugs endowed a weak base moiety, which increased the drug solubility or lipophilicity and permitted the prodrugs to go cross into the aqueous environment, became ionized, and formed complexes with sulfate ions[22−24]. The drugs were delivered to the tumor tissue by the EPR effect, and countered an intricate tumor acidic pH microenvironment. Thereafter, a similar circumstance involved endosomes and lysosomes[25]. Specifically, weak-base drugs became charged and their cellular permeability was decreased. Taking this into account, it was considered that weak-base modified drugs may become ionized in an acidic environment and their penetrability through the lipid-based membrane was inhibited, resulting in a moderate therapeutic efficacy[26−28]. However, the unionized fraction of weak acid drugs increases outside the tumor on account of low pH and easily diffuses through the cell membrane. The significant necessity for the drug to exempt the endocytic pathway trapping suggested superiority of the

enhanced permeability of "liposome-dependent" drugs, many of which are weakly acidic, would be much permeant at an acidic pH of endosomes/lysosomes.

In this study, several poorly water-soluble chemotherapeutic agents containing hydroxyl group, including docetaxel, cabazitaxel, etoposide, combretastatin A4, and podophyllotoxin, were conjugated with anhydride or dicarboxylic acid to confer them with weak acid properties, and then could be actively loaded into liposomes by pH gradients. When compared with Jevtana®, the commercial products of the cabazitaxel, CTX weak-acid derivatives liposomes were further comprehensively evaluated on safety profiles, including systematic toxicity and potential central nerve toxicity. Furthermore, pharmacokinetic studies and *in vivo* biodistribution were conducted. Subsequently, pharmacodynamics assessments were performed by using the prostate carcinoma model and its lung metastatic model. A facile derivatization method of poorly water-soluble drugs by weak acid groups or side chains was introduced, which achieved remote drugs loading into liposomes, then was exploited for their therapeutic potentials.

## 2. Materials and methods

### 2.1. Materials and regents

CTX was purchased from NanJing Jingzhu Bio-technology Co., Ltd. (Nanjing, China). 1,2-Dioctadecanoyl-*sn*-glycero-3-phophocholine (DSPC), cholesterol (for injection, Chol) and 2-distearoyl-snglycero-3-phosphoethanolamine-*N*-[methyl (polyethylene glycol)-2000 (DSPE-PEG2000) were commercially available from Shanghai Advanced Vehicle Technology Pharmaceutical Ltd. (Shanghai, China). Succinic anhydride (SA), glutaric anhydride (GA), *trans*-2-butene-1,4-dicarboxylic acid (DA), *N*-(3-dimethylaminopropyl)-*N*-ethylcarbodiimide hydrochloride (EDCI) and 4-dimethylaminopyrideine (DMAP) were purchased from Aladdin Industrial Corporation (Shanghai, China). Sepharose CL-4B gel was obtained from Beijing Solarbio Corporation (Beijing, China). Roswell Park Memorial Institute (RPMI-1640) and trypsin were purchased from Gibco (Beijing, China). Dulbecco's modified Eagle's medium (DMEM), glucose, and sodium pyruvate were from Thermo Fisher Scientific Inc. (Shanghai, China). Fetal bovine serum (FBS) was from Foundation (Beijing, China), and MTT was purchased from Dalian Meilun Biotech Co., Ltd. (Dalian, China). 96-well plates were supplied by NEST Biotechnology (Wuxi, China). All other reagents were of analytical pure grade.

### 2.2. Synthesis of weak acid drug derivatives

Five sparingly water-soluble chemotherapeutic agents, including docetaxel, cabazitaxel, etoposide, combretastatin A4, and podophyllotoxin, were selected to synthesize several weak-acid derivatives by modification with different length carbon chain dicarboxylic acid, SA, GA and DA. Drug succinic acid and glutaric acid derivatives (SA–D and GA–D) were synthesized by using corresponding anhydride, and drugs with aid of DMAP at a molar ratio of 1.5:1:0.2 in the anhydrous dichloromethane for 24 h. For the drug *trans*-2-butene-1,4-dicarboxylic acid derivatives (DA–D), esterification was performed between the carboxyl group of DA and the hydroxyl group of the drug in the presence of EDCI and DAMP at a molar ratio of 1.5:1:2:0.5. Reactants were dissolved in the anhydrous dichloromethane and the reaction lasted for 40 min at 0 °C, and then the reaction mixture was transferred to room temperature for 2 h. The reaction mixture was processed with 0.5 mol/L HCI to remove DAMP and EDCI. The crude product was purified by preparative high-performance liquid chromatography (pre-HPLC) to obtain a white solid. Target products were confirmed by mass spectrometry (Agilent Technologies Inc., Agilent 1100 Series LC/MSD Trap, Beijing, China) and nuclear magnetic resonance spectroscopy (400 MHz $^1$H NMR, Bruker, Bruker AV-400, Beijing, China). The chemical stability of derivatives was determined in simulative biologic media (mouse plasma) for 24 h at 37 °C.

### 2.3. Remote loading weak acid derivatives into liposomes and characterization of formulations and in vitro release profiles

Blank liposomes were prepared by a thin-film hydration approach[29]. Briefly, DSPC, Chol and DSPE-PEG2000 were dissolved in chloroform, and the solvent was removed by vacuum distillation. The dry lipid film was hydrated by various concentrations calcium acetate at 65 °C for 30 min. Then, the heterogeneous size of multilamellar liposomes was homogenized by successive extrusion through a 400, 200, and 100 nm pore size polycarbonate membrane at 65 °C for 10 times. Subsequently, exchange of the liposomal external phase was accomplished by passing the liposomes through Sepharose CL-4B gel column pre-equilibrated with sodium sulfate solution, and liposomes were diluted to the required concentration of lipid to use. The remote loading of weak acid drug derivatives into liposomes was achieved by co-incubation of the drug (dissolved in ethanol) and blank liposomes at 65 °C for some time, and ethanol was removed by dialysis or tangential flow. The encapsulation efficiency (EE) was determined by size exclusion chromatography by separating unloaded drug and liposomes, and drug content was determined by HPLC (Hitachi, Tokyo, Japan). The size and zeta potential were measured by Zetasizer Nano ZS90 (Malvern, UK). Morphology of the liposomal formulation was observed by transmission electron microscopy (TEM, Hitachi HT7700, Tokyo, Japan) at an operating voltage of 80 kV and cryo-transmission electron microscopy (cryo-TEM, Thermo Fisher Scientific Inc., Talos F200C, Shanghai, China). The liposomes was investigated at 4 and 25 °C for storage.

The *in vitro* release experiments were performed by the dialysis method in the PBS buffer (pH 7.4) media containing 5% ethanol. The various formulations were sealed in the dialysis bags (MW 3500 Da) and placed in the 20 mL release media under the condition of shaking (100 rpm, Jiangsu Changzhou Ronghua Instrument Manufacture Co., Ltd., Changzhou, China) at 37 °C for 72 h. The content of three derivatives of CTX and CTX was detected by HPLC.

### 2.4. Cell culture and animal model

RM-1 (prostate carcinoma) cells and 4T1 (breast cancer) cells were kindly provided by the Stem Cell Bank, Chinese Academy of Sciences. In brief, RM-1 cells were cultured in DMEM containing 50 units/mL streptomycin, 100 units/mL penicillin, and FBS (10%) at 37 °C and 5% $CO_2$. Moreover, 4T1 cells were cultivated

in RPMI-1640 medium containing 50 units/mL streptomycin, 100 units/mL penicillin and 10% FBS at 37 °C and 5% $CO_2$.

Six-week-old male C57BL/6 mice (20 ± 2 g) and Sprague–Dawley (SD) rats (230 ± 20 g) were purchased from Liaoning Changsheng Biotechnology Co., Ltd. (Benxi, China). Animals were raised in a proper environment for experiments. All procedures and experiments were carried out in accordance with the guidelines provided by the Institutional Animal Ethical Care Committee (IAEC) of Shenyang Pharmaceutical University, China.

### 2.5. *Cellular uptake*

The RM-1 cells were seeded into 12-well plates and cultured for 24 h before adding the various formulations. The various formulations (Jevtana®, lipo SA-CTX, lipo GA-CTX and lipo GA-CTX, containing 200 ng/mL CTX) were co-incubated with cells for 4 or 8 h. After treatment, the cells were washed by cold PBS and collected. The cells were sonicated, centrifugated, and the supernatant were reserved and then drugs were determined by UPLC–MS/MS method (Waters Co., Ltd., Milford, MA, USA).

### 2.6. *Cytotoxicity evaluation*

CTX weak-acid derivatives were further studied including: cabazitaxel succinic acid derivative (SA-CTX), CTX glutaric acid derivative (GA-CTX) and CTX *trans*-2-butene-1,4-dicarboxylic acid derivative (DA-CTX).

Evaluation of the cytotoxicity against RM-1 and 4T1 cells was performed by using the MTT assay. Tumor cells were seeded into 96-well plates before drug treatment. After 24 h of pre-incubation, RM-1 cells were treated with serial dilutions of Jevtana®, SA-CTX, GA-CTX, DA-CTX, and corresponding liposomes of the latter three were incubated for 48 and 72 h. Untreated cells served as controls. At the end of treatment, 20 μL of MTT solution (5 mg/mL) was added to each well, and cells were incubated for 4 h at 37 °C. In addition, 4T1 cells were seeded into 96-well plates at a density of $1 \times 10^3$ per well and drug treatment was the same as RM-1 cells. After 4 h of co-incubation with MTT solution, the medium was discarded and 200 μL DMSO was added, shaken in the dark and the absorbance of the solution was measured in a microplate reader at 490 nm. Each concentration was tested in six wells and data were presented as the mean ± SD.

### 2.7. *Pharmacokinetics and biodistribution*

Sprague–Dawley rats (230 ± 20 g) were randomly divided into five groups ($n = 5$ per group). Jevtana®, SA-CTX liposome (lipo SA-CTX), GA-CTX liposome (lipo GA-CTX), DA-CTX liposome (lipo DA-CTX) were intravenously administrated with an equivalent dosage of 5 mg/kg of CTX. At defined time intervals, about 300 μL blood was collected and centrifuged ($1.2 \times 10^4$ rpm, 5 min, Shanghai Anting Scientific Instrument Factory, TGL-16B, Shanghai, China) to obtain plasma. The concentration of CTX and three derivatives in plasma was determined by a validated UPLC–MS/MS method.

A subcutaneous RM-1 prostate cancer (PCa) model was established in male C57BL/6 mice by subcutaneously transplanting $5 \times 10^6$ RM-1 cells suspended in 200 μL PBS into the right flank region. Thirty-six tumor bearing C57BL/6 mice were stochastically divided into four groups when the tumor volume reached approximately 200 $mm^3$ ($n = 3$). Jevtana® and the three CTX weak-acid derivatives liposome formulations were injected *via* the caudal vein at a dose equivalent to 6 mg/kg of CTX. At the timed intervals, mice were sacrificed and their major organs were harvested, rinsed carefully with saline, weighed, and stored at −20 °C until analysis. The tissues concentration of weak acid derivatives and free CTX was measured by UPLC–MS/MS.

### 2.8. *Maximum tolerated dose and safety profile assessment*

The maximum tolerated dose (MTD) of drugs in healthy C57BL/6 mice and SD rats was determined by using a multidose scheme and was identified as the maximum dose of a drug or formulation that did not induce humane endpoints during treatment, where the MTD was the highest nonlethal deliverable dose, and less than 20% weight loss was used as humane endpoints. During the trials, the body weight of animals was monitored. When reaching humane endpoints, mice were sacrificed and the whole blood and serum were collected. Hematology and serology were tested. Major organs (heart, liver, spleen, lung, and kidney) were harvested, fixed in 4% formalin, and assessed by hematoxylin–eosin (H&E) staining. Cortex and hippocampus were removed, carefully rinsed with PBS, and further evaluated by H&E staining and immunofluorescence.

### 2.9. *In vivo antitumor efficacy assay*

A subcutaneous RM-1 prostate tumor model was established as mentioned above to estimate the antitumor efficacy of CTX weak-acid derivatives remote loading liposomes and compared to Jevtana®. When the tumor volume reached 100–150 $mm^3$, mice were randomly divided into 8 groups as follows: saline, Jevtana®, low dose at 6 mg/kg and high dose at 30 mg/kg equivalent dosage of CTX: lipo SA-CTX, lipo GA-CTX, and lipo DA-CTX, and mice were treated every three days with various formulations *via* tail vein. The dose of CTX was based on the results of the MTD test. When the tumor volume was above 2000 $mm^3$, mice were sacrificed and tumor tissues were collected for H&E staining and TUNEL staining. Serum was collected. The prostate-specific antigen (PSA) level in serum and tumor tissue was determined by ELISA kit (Shanghai Jianglai Industrial Limited by Share Ltd., Shanghai, China).

A pseudo-metastases model in the lungs of RM-1 prostate cancer was established according to previous methods[30]. At 48 h after the injection of tumor cells *via* tail vein, various formulations were administrated to treat prostate cancer lung metastasis. The administration scheme and dose were the same as in the subcutaneous prostate tumor model. Body weight was recorded. Some of the mice were sacrificed and lungs were dissected, weighed, stained with Bouin's fixative solution, the number of foci were counted, and the pathological changes of lungs were assessed by H&E staining.

### 2.10. *Statistical analysis*

Data were calculated and presented as the mean ± SD. Comparison among groups was analyzed with Student's *t*-test and one-way analysis of variance (ANOVA), and $P < 0.05$ was considered statistically significant.

## 3. Results and discussion

### 3.1. *Weak acid drug derivatives synthesis and preparation of remote loading liposomes*

Upon the state of the art of liposome technology, the next milestone of liposomology was achieved by leading the way of remote loading of water-insoluble drugs. Some methods were developed but limitation remained. As far as we are concerned, fascicle chemical modification or derivatization of drugs were effective on developing remote poorly water-soluble drugs loading into liposomes. Previously, weak base moieties were attached to docetaxel or gemcitabine to realize active loading[22,23]. On the contrary, we tried to modify sparingly water-soluble drugs with weak acidic moieties and then the weak acid drug derivatives (Fig. 1A) were remotely loaded into the liposomal aqueous core by a calcium acetate gradient method (Fig. 1B) and retained. The symbolic structure of the weak acid drug derivate contained the following parts: drugs (docetaxel, cabazitaxel, etoposide, combretastatin A4, and podophyllotoxin are shown in Supporting Information Fig. S1A–S1E), the linker (carboxylic acid ester bond used in this research), spacers, and the carboxyl group. The linker is a connection bond between drugs and weak acid moieties. The carboxyl ester bond was chosen as a linker in that anhydride and dicarboxylic acids were used as weak acid moieties in this scenario (Fig. S1F–S1H). Other types of connection bonds might also be introduced with homologous binary acids or anhydride by simple synthesis, including ether bond, carbamate, carbonate bond, boronate ester, phosphate ester, and sulfate ester, to adjust the activity of derivatives[31]. Several important organic acids may be introduced, such as succinate. Succinate is an intermediate metabolite in the tricarboxylic acid cycle and plays a crucial role in the formation of mitochondrial ATP, and serves as a metabolic signal in inflammation, which can promote inflammation and play an important role in the cancer immune cycle[32,33], that deserves further investigation. Promising small molecule organic acids were attached to chemotherapy drugs, which would play dual roles in the drug delivery system. A spacer adjusted the log*P* of derivatives, strength of acid or stability of the linker on demand. A series of poorly water-soluble drugs derivatives were successfully synthesized which were verified by MS and $^1$H NMR listed in Supporting Information. The synthesis of the therapeutic agents' weak acid derivatives was fascicle and the yield was high. The purification of crude products was easy.

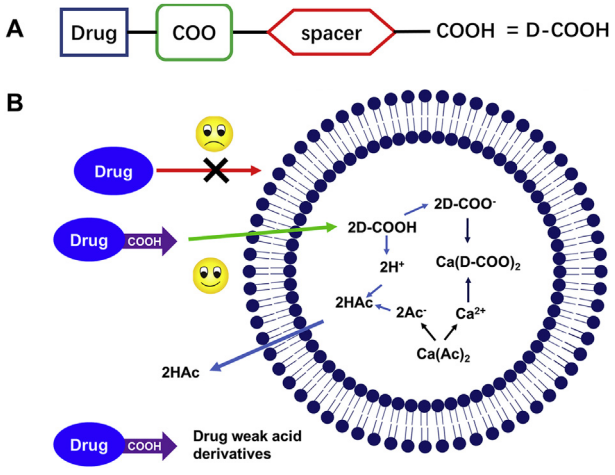


**Figure 1** (A) Illustration of drug weak acid derivatives. (B) Remote loading drug weak acid derivatives into liposomes by pH gradient.

The drugs loaded by calcium acetate gradients required the following: log*D* in the range of −2.5 to 2 at pH 7 and p$K_a$>3 for amphipathic acid[34]. The solvent-assist-loading technology had an outstanding performance on active loading ionizable water-insoluble molecules, implying that log*D* no longer had a decisive restrictive character for developing remote loading liposomes. We tested the ability of drugs derivatives entering liposomes and retained in the aqueous core. The lipid composite of formulation was referred to Onivyde®, with a relative content higher of Chol but lower of DSPE-PEG2000 to prevent accelerated blood clearance (ABC)[24]. High phase-transition (high $T_m$) phospholipids were employed, such as distearoyl or hydrogenated phosphatidylcholines (PC) and inclusion Chol, to reduce drug leakage and liposome clearance by the mononuclear phagocyte system (MPS) by decreased binding of plasma opsonins[15]. Three CTX weak acid derivatives (as presented in Fig. 2A) were capable of being loaded into liposomes with a high EE (>95%), small size (120−140 nm), and narrow PDI (<0.1, Supporting Information Fig. S3), but behaved somewhat different in formulations of some aspects presented in Fig. 2B and C. The differences in D:L were mainly under the influence of p$K_a$ of derivatives modified by different weak acids (p$K_a$: SA < DA < GA). The zeta potential of three liposomes was nearly neutral and consistent about −4.5 mV, due to the same lipid composition. All CTX derivatives demonstrated a similar stability during the remote drug loading (Fig. S4A and S4B), however, a different storage stability was observed (Fig. S4C and S4D). The DA-CTX liposomes displayed good stability at 4 °C for three weeks. However, DA-CTX liposomes were relatively unstable for a decreased EE of about 10% on Day 14 at 25 °C. The existence of a pH gradient was vital for the remote loading drug weak acid derivatives into liposomes. There was a very small fraction of the weak acid derivatives that passively diffused into liposomes assisted by miscible solvents, even if a high ratio of miscible solvents was used (Fig. S4E and S4F). Other drugs simply modified with weak acids could be loaded into liposomes by using the pH gradient method as shown in Supporting Information Table S1. The EE of all derivatives ranged 80%−96%. Cyro-TEM micrograph of lipo SA-CTX (Fig. 2D) clearly shows that SA-CTX appeared as an electron-dense precipitate within aqueous liposomal interior. The results indicate that the drugs weak acid derivation method could be applied to enable therapeutic agents containing a modifiable hydroxyl active loading into liposomes.

The *in vitro* release profiles of CTX weak acid derivatives loaded liposomes are shown in Supporting Information Fig. S5B. The sustained release profiles of all formulations were observed. And the significant difference in release behaviors are demonstrated between lipo GA-CTX and lipo SA-CTX or lipo DA-CTX, probably due to the different lipophilicity of CTX derivatives and different D:L ratios[35,36]. The most drugs were released from lipo GA-CTX, and meanwhile most CTX was released from lipo GA-CTX. Only a small amount drugs were released from lipo SA-CTX and lipo DA-CTX (<20%), and little CTX was released.

### 3.2. *Cellular uptake and cytotoxicity evaluation*

The cellular uptake of CTX, its derivatives and corresponding liposomes was investigated at different time by UPLC–MS/MS. The *in vitro* drug cellular uptake was a time-dependent manner (Supporting Information Fig. S6). The CTX solutions entered

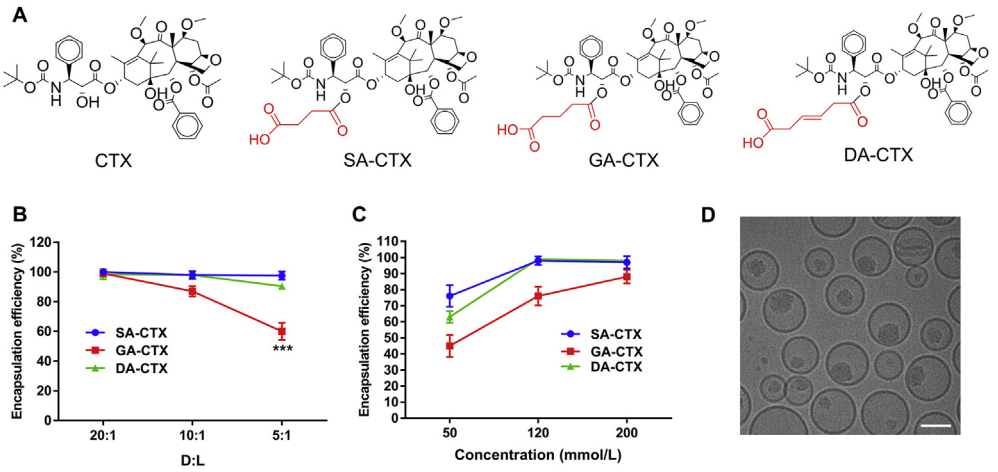


**Figure 2** The properties of liposomes. (A) The structures of cabazitaxel and its weak acid derivatives. The effect of drug-to-lipid (D:L) (B) and inner aqueous phase concentration (C) on encapsulation efficacy. (D) The cryo-TEM image of lipo SA-CTX. Data are shown as the mean ± SD, $n = 3$, $^{***}P < 0.001$. Scar bars = 50 nm.

cytoplasm easily and quickly by passive diffusion, showing CTX was the most content in cytoplasm at 2 h. The liposomes entered cytoplasm by endocytosis, which was slower than passive diffusion of CTX solution, thereby compromising the uptake of drugs at different timepoints. Interestingly, the uptake of CTX weak acid derivatives was less than that of the corresponding liposomes. It was suspected that the CTX weak acid derivatives ionized in the neutral cultured medium, resulting in the low permeability than its molecular state.

The activity of weak acid derivatives of drugs was associated with potential therapeutic effects. Jevtana® has been used in metastatic castration-resistant prostate cancer (mCRPCa) given that it was superior in the activity compared to other taxanes and the ability of overcoming P-gp-mediated taxane resistance[37]. The CTX weak acid derivatives were further evaluated in prostate carcinoma (RM-1 cells) and breast cancer (4T1 cells). All three CTX weak acid derivatives presented time- and concentration-dependent cytotoxicity over RM-1 cells, but tended to decrease cytotoxic activity when compared to Jevtana® as demonstrated by the $IC_{50}$ shown in Fig. 3. The $IC_{50}$ of CTX derivatives (DA-CTX < SA-CTX < GA-CTX) existed apparent divergence resulting from the difference among structures. When the derivatives were loaded into liposomes, the inhibitory effect on cell proliferation was significantly enhanced when compared to its free form. It was considered that these results were due to the differences in cellular uptake (Fig. S6) and intracellular transport. In neutral 1640 medium, the ionized states of free drugs dominated compared to the molecular states, resulting in low cell permeability. The liposomes were mainly ingested into cells by endocytosis, and then subsequently trapped in lysosomes. The released

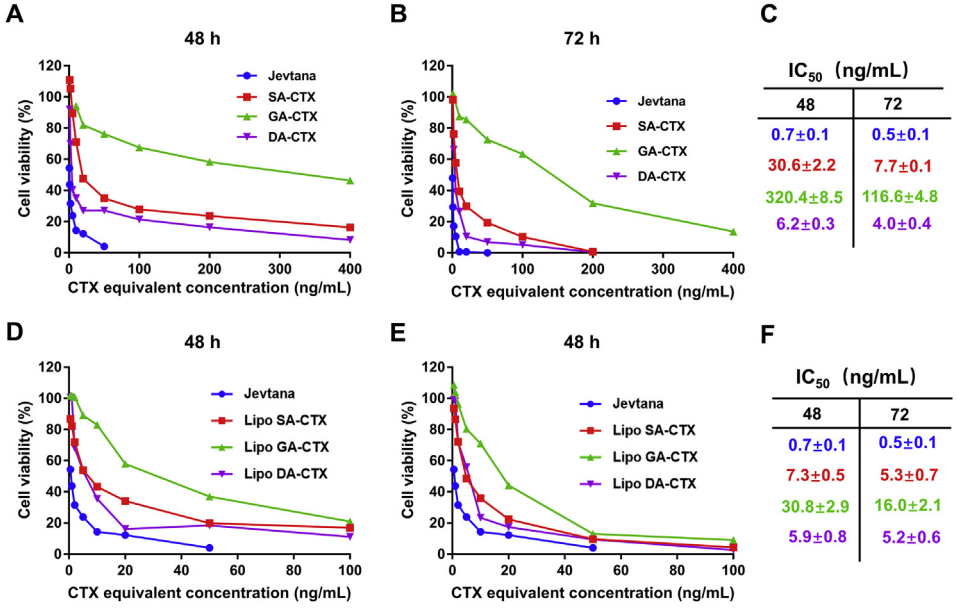


**Figure 3** The cytotoxicity evaluation. The cytotoxicity of Jevtana, cabazitaxel weak acid derivatives and its liposome formulations at 48 and 72 h. Data are shown as the mean ± SD, $n = 6$.

weak acid derivatives readily escaped from the acid environment by molecular state forms to exert work. Similar results were observed in 4T1 cells (Fig. S7).

### 3.3. *Pharmacokinetics profile and in vivo biodistribution*

Healthy SD rats were used to evaluate the pharmacokinetic profiles of CTX weak acid derivatives liposomes following intravenous administration. For direct comparison of different liposomes formulations, the pharmacokinetic parameters are summarized in Supporting Information Table S2. As shown in Fig. 4A, CTX in Jevtana® was rapidly cleared. In comparison, three liposomes display a remarkably prolonged blood circulation time. The area under the curve ($AUC_{0-t}$) values of lipo SA-CTX, lipo GA-CTX, and lipo DA-CTX are 841.8-, 781.7-, and 976.5-fold higher compared to that of Jevtana®, respectively (Table S2). The released CTX from derivatives is shown in Fig. 4B, and it is found that the lipo SA-CTX released less CTX than lipo GA-CTX and lipo DA-CTX for its higher D:L (1:5 *vs.* 1:20 or 1:10)[15], which was consistent with *in vitro* release profiles. The released CTX from lipo GA-CTX and lipo DA-CTX has similar profiles. Interestingly, the concentration of CTX released from lipo GA-CTX and lipo DA-CTX increased after an initial decrease, and then tended to decline with time, which was likely because CTX derivatives gradually converted to a CTX form in the inner aqueous environment. When compared with other previously reported CTX formulations, remote drugs loading liposomes have excellent pharmacokinetic properties[37].

The biodistribution of derivatives and CTX were investigated in PCa-bearing C57BL/6 mice. The drug concentration of the targeting tissue (tumor) and non-targeting tissue (heart, liver, spleen, lung, kidney, and brain) are presented in Fig. 4C and D and Supporting Information Fig. S8. Lipo GA-CTX had the lowest concentration at the tumor tissue and a higher concentration in the brain. Moreover, the concentration of DA-CTX in all tissues was higher than other formulations, especially in tumor tissue, which was partly due to a higher total $AUC_{0-t}$. The chemical stability of three derivatives of CTX was investigated in biologic media (mouse plasma). As shown in Fig. S4A, the better chemical stability of DA-CTX meant longer $t_{1/2}$, though more DA-CTX may release from Lipo DA-CTX. The interaction between DA-CTX and plasma proteins may prevent the DA-CTX from degradation, contributing to longer circulation time and the more distribution in all the tissues. However, the exact underlying mechanism remained further investigation. The CTX released from various liposomes presents a different elimination speed as illustrated in Fig. 4D. A more rapid elimination of Jevtana® was found in both plasma and tumor tissue when compared to liposomes. The concentration of CTX from lipo SA-CTX and lipo DA-CTX in the tumor was significantly higher compared to that of Jevtana® and lipo GA-CTX after a single dose administration, which was indicative of a better antitumor efficiency. Macrophages rather than parenchymal cells contributed to the majority of uptake of liposomes in the liver and spleen over other organs, which was a common outcome that emerged in nano drug delivery systems[38]. Non-targeting tissues exposed directly to Jevtana®, including heart, spleen, and kidney, could cause damage to corresponding sites.

### 3.4. *Maximum tolerated dose and safety profile assessment*

Prior to antitumor efficacy experiments, both of the MTD and safety profile were evaluated, that were the pivotal factor to balance the efficacy and safety profiles of anticancer drugs or

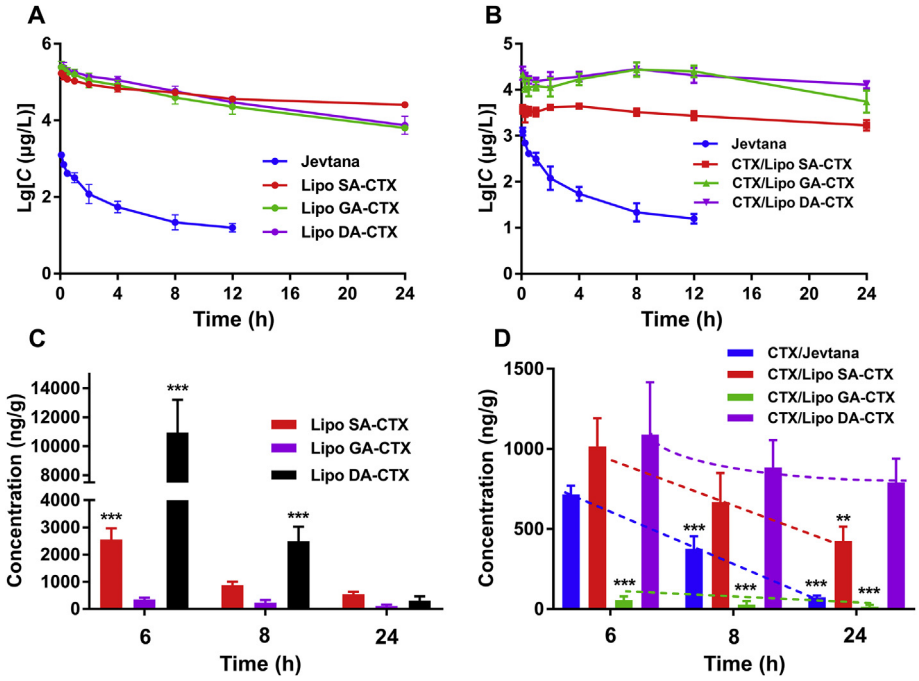


**Figure 4** The pharmacokinetics and biodistribution of liposomes. (A) The pharmacokinetics of Jevtana and cabazitaxel weak acid derivatives liposomes. (B) The concentration of cabazitaxel (CTX) profiles released from Jevtana and corresponding liposomes. (C) and (D) The biodistribution of CTX and its weak acid derivatives in tumor tissue at different time points. Dashed lines represent trends in drug content. Data are shown as the mean ± SD, A&B, $n = 5$; C&D, $n = 3$, $^{**}P < 0.01$, $^{***}P < 0.001$.

formulations. C57BL/6 mice and SD rats were used to implement experiments with a multidose scheme (Fig. 5A), and behaviors and body weight of mice and rats were observed and recorded. Jevtana® (CTX dissolved in Tween 80 and ethanol) was approved by the U.S. Food and Drug Administration (FDA) for mCRPCa at a dose of 25 mg/m$^2$ every three weeks, combined with 10 mg of orally administrated prednisone daily to reduce side effects[37]. In mice, we utilized 6 mg/kg at an initial dose that was approximatively equivalent to the dose used in humans. Mice that received a Jevtana® injection at a dose of 8 mg/kg were gradually emaciated after the third dose and a mean reduction in body weight of mice was more than 20% (Fig. 5B), while liposomes were tolerated until the dose exceeded 30 mg/kg. Overt improvement in the MTD was related to the enhancing therapeutic index (TI), which was defined as the ratio of MTD to minimum effective dose (MED), decreasing the risk of adverse reactions with elevated doses during the treatment. The results of hematology and serum analysis of mice demonstrated that Jevtana® caused significant neutropenia, leukopenia, and obvious creatinine (CR) augmentation (Fig. 5C and D), indicating potential toxicity on the marrow and kidney because of unnecessary biodistribution. Fibrosis was observed in the spleen harvested from the Jevtana®-treated group (Fig. S9). Other indices with no significant differences are shown in Supporting Information Fig. S10 and Table S3. Toxicity of major organs was evaluated by H&E staining (Fig. S9) at various tolerated doses. When SD rats were administrated 6 mg/kg, significantly more severe adverse reactions occurred in the Jevtana® group after the third dose (Fig. S11). Apart from the loss of body weight, diarrhea, and hypokinesia were observed, while these adverse events were not observed in the liposomes-treated groups. These results indicated an advantageous safety profile of liposomes compared to Jevtana®.

Considering the increasing number of long-term cancer survivors, it is critical to address the extent, persistence, and neuropathologic mechanisms underlying chemotherapy-related cognitive decline or the "chemobrain" that originates from central nerve system toxicity, damage, and lesions[39,40]. The study found that mice became dull and less active probably because of potential central nerve toxicity and impaired cognitive function. Analogous phenomena were not observed in the liposomes group. CTX possessed superior ability to pass the blood–brain–barrier (BBB) in contrast to first generation taxanes. Previous studies reported that CTX caused dose-dependent central nervous system toxicity in rats at doses from 0.5 to 1.5 mg/kg[41]. Therefore, it was

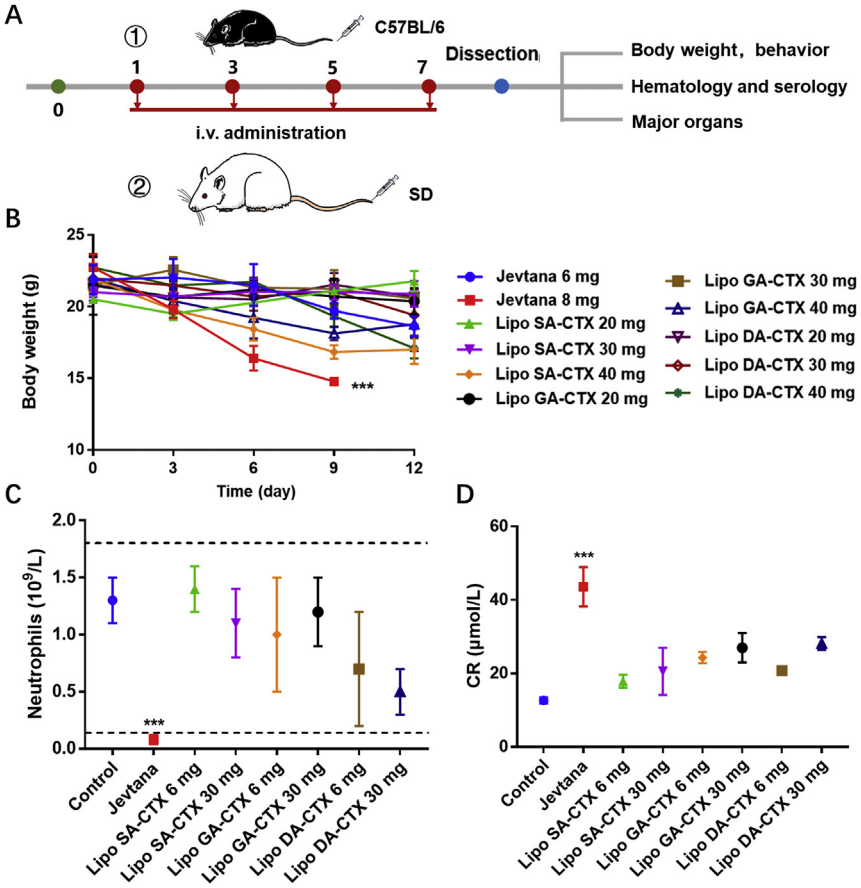


**Figure 5** The safety evaluation of various formulations. (A) The scheme of safety assay. (B) The maximum tolerated dose (MTD) of various formulations in C57BL/6 mice. (C) Neutrophil levels of various groups after formulations administration. (D) Creatinine (CR) levels of various groups after administration. Data are shown as the mean ± SD, $n = 3$, ***$P < 0.001$.

necessary to evaluate the safety profiles on the central nervous system when using higher dosage. The decline of the CTX concentration in the brain was slower compared to that in the tumor and plasma (Fig. 4 and Fig. S8), probably resulting in impairment to the brain. Pyknotic nuclei and eosinophilic necrosis (arrow in white) and heteromorphic nuclei (arrow in green) were easily observed in the cortex after Jevtana® treatment (Fig. 6). A similar phenomenon was observed when using high doses of lipo GA-CTX and lipo DA-CTX at 30 mg/kg due to accumulated cytotoxicity of the drug, although no abnormal behavior was observed during the experiments. Microglia activation ($Iba1^+$) was found, indicating a potential inflammatory signature (Fig. 6). The neuroinflammation caused by cytotoxic treatment may bring about neurodegenerative disease[42]. Immature neurons ($DCX^+$) and mature neurons ($Neun^+$) in the hippocampus were detected to assess the impact of chemotherapy on neurogenesis (Fig. 6). The significant decrease of fluorescence signals in Jevtana®-treated and lipo GA-CTX-treated animals suggested that CTX treatment damaged neurogenesis. The chemobrain was the result of impairment of the cortex and hippocampus. Among various formulations, lipo SA-CTX had a better safety profiles within the scope of this study. Moreover, the CTX released from lipo GA-CTX was increased compared to other formulations from 6 to 48 h (Fig. S8), which may be beneficial to the brain tumor therapy.

### 3.5. *In vivo antitumor efficacy*

Many drugs for treating mCRPCa were limited for clinical practice accounting for intrinsic or acquire resistance by overexpression of P-glycoprotein (P-gp) and/or unacceptable dose-limiting side effects[43]. CTX, a second-generation taxane, has intrinsic abilities to overcome P-gp-mediated taxane resistance[37]. The antitumor activity of CTX weak acid derivatives liposomes was investigated in a RM-1 subcutaneous tumor model and compared to Jevtana® (Fig. 7). Tumor growth curves are presented in Fig. 7B. The tumor volume of the saline group expanded rapidly when compared to others. All formulations had an inhibitory effect on tumor growth. However, after terminating treatment, retardant tumor growth resumed in the Jevtana® group, low dose liposomes group, and high dose lipo GA-CTX group. No differences were observed when the CTX equivalent dosage was set to 6 mg/kg; however, the body weight of mice rapidly decreased upon receiving Jevtana® therapy (Fig. 7C). A higher dose of therapeutic agents delivered by liposomes showed pronounced antitumor efficacy when administrating lipo SA-CTX and lipo DA-CTX. The halted tumor growth lasted for 30 days. Mice treated with a high dose of lipo SA-CTX and lipo DA-CTX prolonged a median overall survival time that was longer than that of other groups (Fig. 7E), under

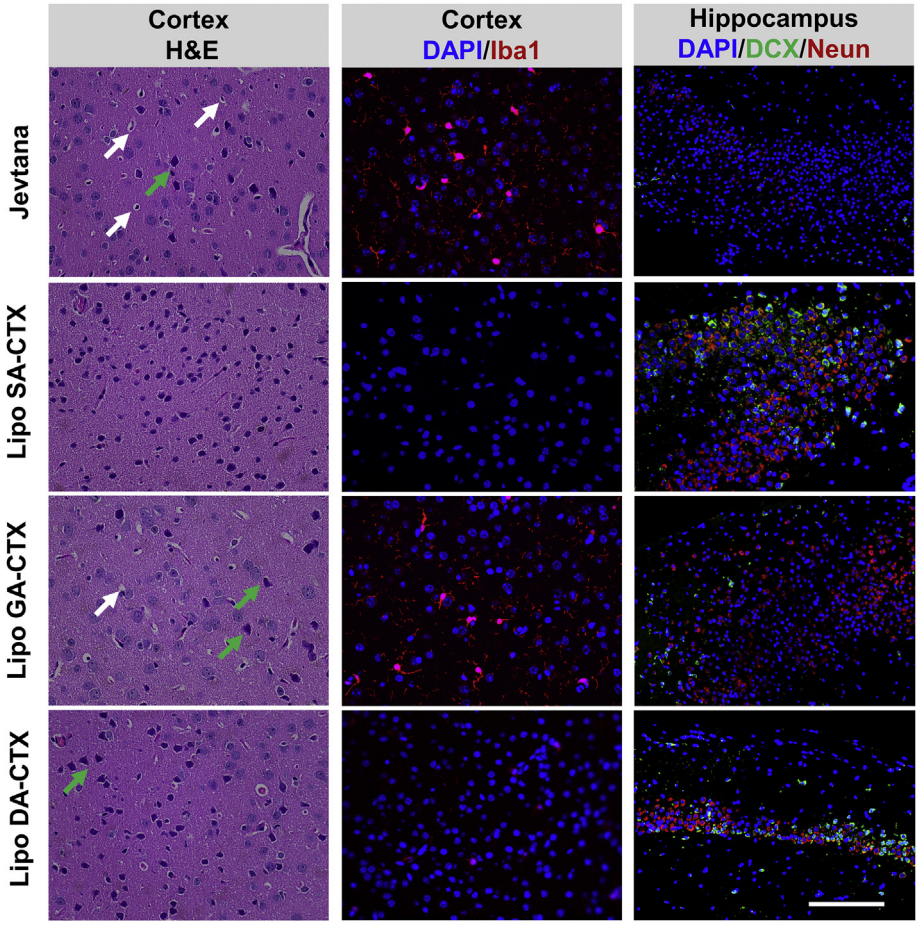


**Figure 6** The safety profiles of various formulations at a tolerated dose on central nervous system assessed by hematoxylin and eosin (H&E) staining and immunofluorescence analysis. Pyknotic nuclei and eosinophilic necrosis were indicated by arrows in white and heteromorphic nuclei was indicated by arrows in green. Activated microglia ($Iba1^+$) in red are shown in the middle panel. Doublecortin ($DCX^+$), representing immature neurons, was stained in green. Neuron-specific nuclear antigens ($Neun^+$), indicating mature neurons, were stained in red. Scar bar = 100 μm.

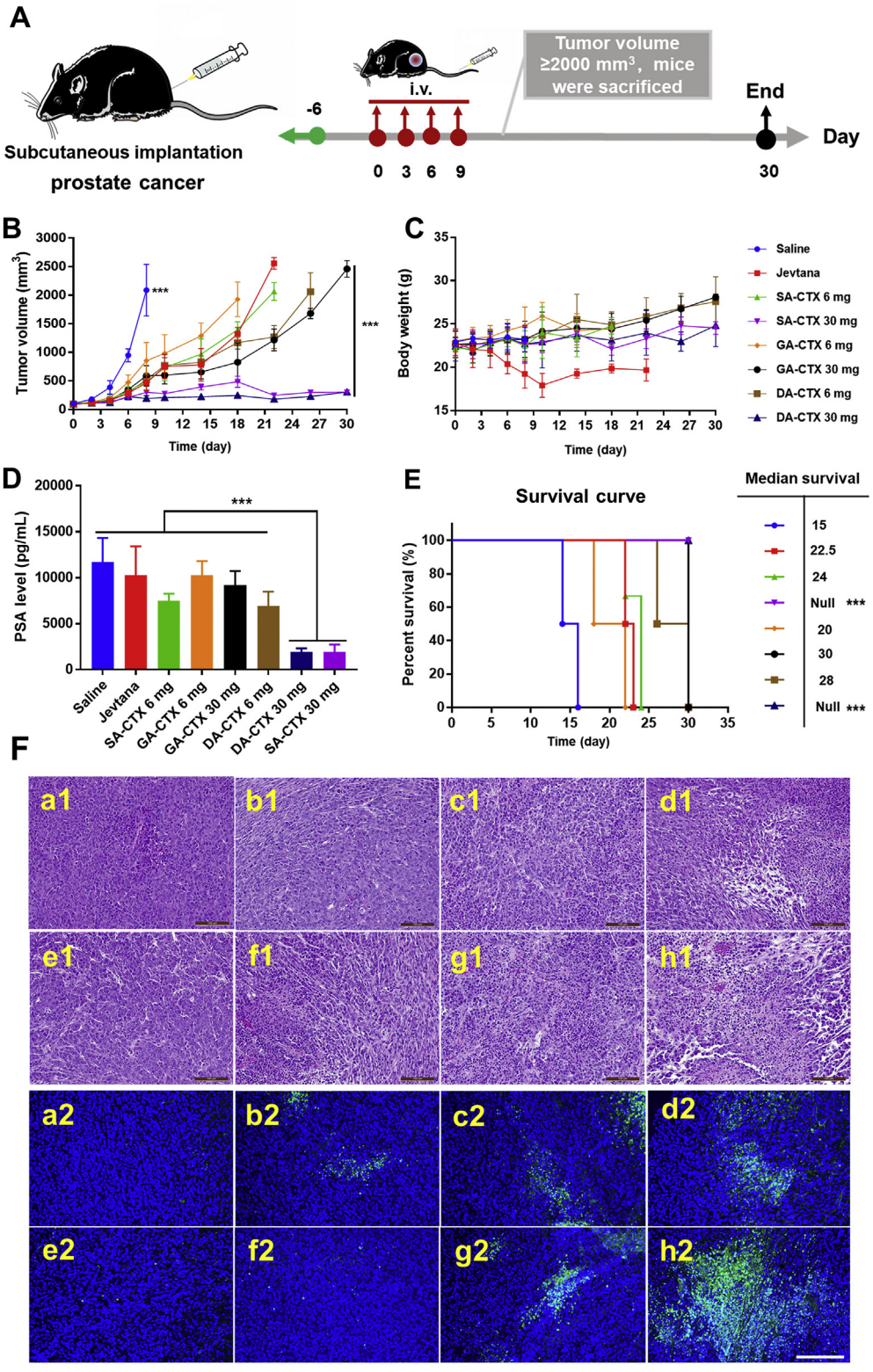


**Figure 7** The antitumor efficacy of various formulations. (A) The experimental scheme of formulations against prostate cancer. (B) Tumor growth curves. (C) Body weight curves. (D) Serum prostate-specific antigen (PSA) levels after treatment. (E) Corresponding survival curves and median survival periods to panel (A). (F) Typical hematoxylin and eosin (H&E) (1) and TUNEL (2) staining of tumor tissues after treatment. In panel E&F, a-Saline, b-Jevtana, c-Lipo SA-CTX 6 mg/kg, d-Lipo SA-CTX 30 mg/kg, e-Lipo GA-CTX 6 mg/kg, f-Lipo GA-CTX 30 mg/kg, g-Lipo DA-CTX 6 mg/kg, h-Lipo DA-CTX 30 mg/kg. Data are shown as the mean ± SD, $n = 6$, $^{*}P < 0.05$, $^{**}P < 0.01$, $^{***}P < 0.001$. Scar bar = 100 μm.

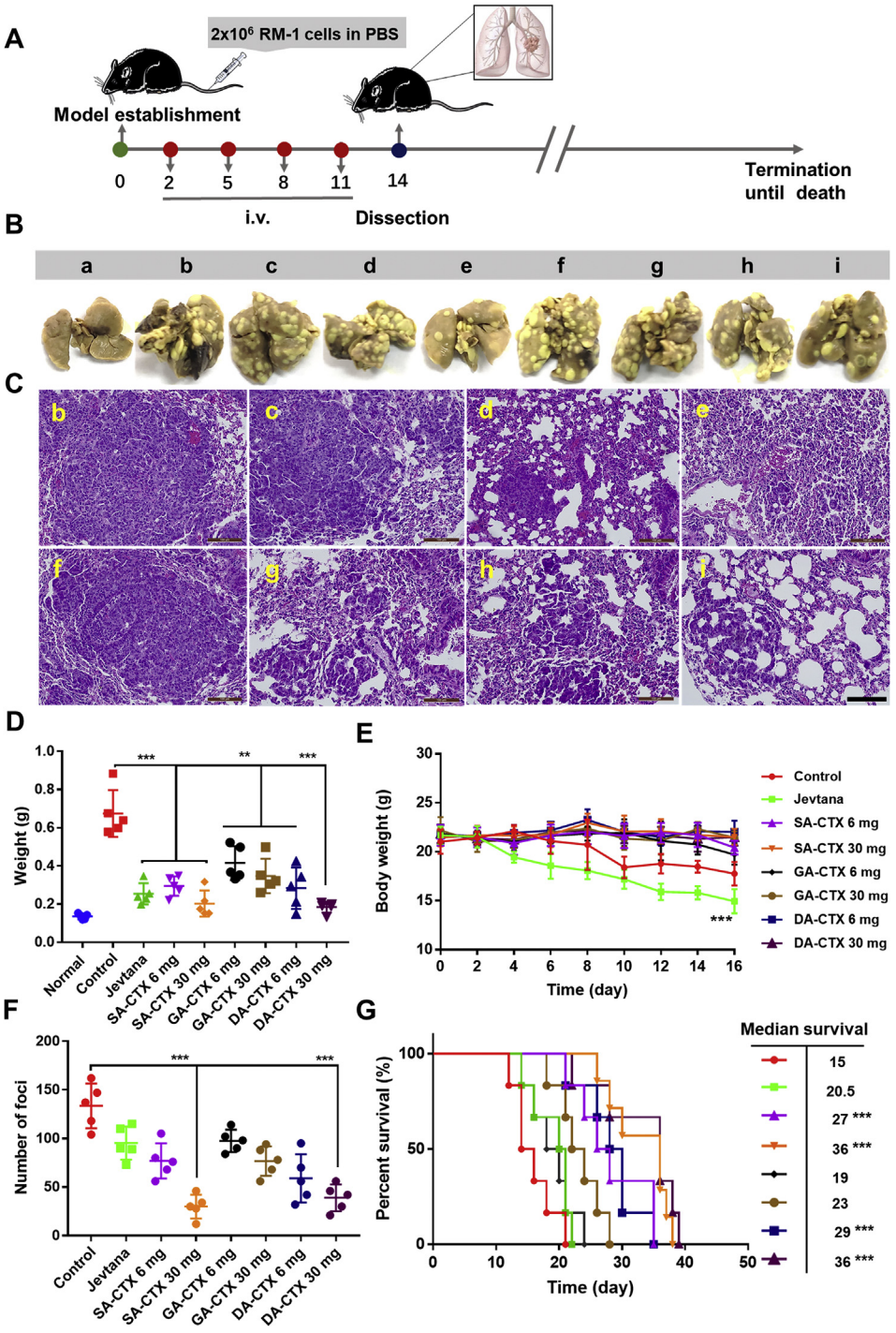


**Figure 8** Pharmacodynamics of various formulations in circulating tumor cells in a lung metastasis model. (A) Model establishment and treatment. (B) Representative images of lungs originated from mice in different groups. (C) Hematoxylin and eosin (H&E) staining corresponding to panel B. (D) The weight of lungs harvested from mice on Day 14 after injection of cancer cells. (E) Body weight changes with time. (F) The number of foci on lungs dissected from mice of different groups. (G) The survival curve and median survival time of different groups. In image B&C, a-Saline, b-Jevtana, c-Lipo SA-CTX 6 mg/kg, d-Lipo SA-CTX 30 mg/kg, e-Lipo GA-CTX 6 mg/kg, f-Lipo GA-CTX 30 mg/kg, g-Lipo DA-CTX 6 mg/kg, h-Lipo DA-CTX 30 mg/kg. Data are shown as the mean ± SD, $n = 5$, $^{**}P < 0.01$, $^{***}P < 0.001$. Scale bar = 100 μm.

conditions that the endpoint was recognized when the tumor volume was larger than 2000 $mm^3$. H&E staining and TUNEL results are shown in Fig. 7F, and present a different degree of necrosis and apoptosis of tumor tissue, with the lowest degree of saline and the highest degree of lipo SA-CTX 30 mg/kg and lipo DA-CTX 30 mg/kg. Serum prostate-specific antigen (PSA) levels are extensively recognized as a biomarker refereed to PC diagnosis, progression, and prognosis responding to systemic

therapies[43,44]. After treatment, PSA levels dropped dramatically in lipo SA-CTX and lipo DA-CTX groups ($P < 0.001$, Fig. 7D), while Jevtana® treatment had an inferior impact on decreasing PSA levels ($P < 0.05$), and lipo GA-CTX at a high dose showed a moderate effect ($P < 0.01$). Low-levels of PSA indicated a favorable prognosis, but tumor growth continued other than high dose lipo SA-CTX and lipo DA-CTX. Only high doses of lipo SA-CTX and lipo GA-CTX showed permanent tumor inhibition.

Pseudo-metastasis in the lungs of RM-1 prostate cancer caused by circulating tumor cells was established to estimate the antimetastatic effects of liposomes (Fig. 8A). At 48 h after intravenous injection, various formulations were administrated to remedy cancer metastatic mice. On Day 14 after injection of tumor cells in vein, mice were sacrificed and lungs were harvested, weighed, and the number of foci was counted. The weight of lungs treated with saline increased significantly compared to those of healthy mice, indicating successful establishment of the model. The rest of the mice were observed. High dose lipo SA-CTX and lipo DA-CTX significantly decreased the number of foci in contrast to others (Fig. 8F), and representative pictures are presented in Fig. 8B, and roughly corresponded to the decrease tendency in the lung weight (Fig. 8D). Overall survival was prolonged after treatment by liposomes except for lipo GA-CTX at a dose of 6 mg/kg. Jevtana® and CTX weak acid derivatives liposome formulation delayed lung metastasis to different degrees. Engorged blood flow provided a chance for circulating tumor cells settlement and metastasis formation[45]. Simultaneously, long circulation liposome formulations had more opportunities to deliver therapeutic drugs to inhibit formative metastasis.

## 4. Conclusions

In this study, weak acid drug derivatives, which could be remotely loaded into the aqueous core of liposomes, were designed. The successful encapsulation of weak acid drug derivatives into liposomes verified our conception. In further studies, we comprehensively evaluated the safety profiles of CTX weak acid derivatives liposomes. Outstanding PK and biodistribution profiles were beneficial to reduce side effects and guarantee therapeutic effects. In the range of tolerated doses, liposomes had a small chance of developing symptoms of hypersensitivity, neutropenia, leukopenia, and nephrotoxicity. Liposome formulations showed no potential central toxicity when compared to Jevtana®, implying that "chemobrain" was avoided to improve patient's prognosis. Compared to Jevtana®, prominent advantages of liposomes were confirmed by reducing the potential toxicity on central nervous system. The MTD accomplished by loading drug into liposomes was elevated, representing a reduced risk in the clinic. Improving the MTD is extremely meaningful to enhance the TI. The antitumor effect of potent lipo SA-CTX and lipo DA-CTX was satisfactory when administrating high doses, however safety profile results suggested that lipo SA-CTX was better than lipo DA-CTX. No significant differences were observed in cancer therapy when compared with Jevtana® at a similar dose. More potential value of "bad drugs" delivered by liposomes was exploited to make the best of them. Weak acid drug derivatives are facilely synthesized and flexibly designed on demand, and could be utilized by remote drug loading liposomes.

## Acknowledgments

This study was financially supported by the National Nature Science Foundation of China (U1608283) and the Career Development Program for Young and Middle-aged Teachers in Shenyang Pharmaceutical University.

## Author contributions

Yongjun Wang and Dan Liu designed, conceived, guided, and funded the investigation. Shuang Zhou performed the major experiments, analyzed the data, processed the figures, and wrote the manuscript. The weak acid drug derivatives were synthesized by the Shuang Zhou, with the help of Jinbo Li, Jiang Yu, Xiao Kuang and Liyuan Yang. The Zhenjie Wang guided the liposomes preparation and characterization. The Shuang Zhou and Jinbo Li conducted the safety evaluation, cytotoxicity experiments, antitumor efficiency assay. The pharmacokinetics and *in vivo* biodistribution were accomplished with the help of Jinbo Li, Jiang Yu, Yingli Wang. Guimei Lin, Hongzhuo Liu and Zhonggui He reviewed and instructed the article. All authors contributed and approved the manuscript.

## Conflicts of interest

The authors have no conflicts of interest to declare.

## Appendix A. Supporting information

Supporting data to this article can be found online at https://doi.org/10.1016/j.apsb.2020.08.001.

## References

1. Rautio J, Kumpulainen H, Heimbach T, Oliyai R, Oh D, Järvinen T, et al. Prodrugs: design and clinical applications. *Nat Rev Drug Discov* 2008;**7**:255–70.
2. Rautio J, Meanwell NA, Di L, Hageman MJ. The expanding role of prodrugs in contemporary drug design and development. *Nat Rev Drug Discov* 2018;**17**:559–87.
3. Zeineldin R, Syoufjy J. Cancer nanotechnology: opportunities for prevention, diagnosis, and therapy. *Methods Mol Biol* 2017;**1530**:3–12.
4. Xie X, Zhang Y, Li F, Lv T, Li Z, Chen H, et al. Challenges and opportunities from basic cancer biology for nanomedicine for targeted drug delivery. *Curr Cancer Drug Targets* 2019;**19**:257–76.
5. Golombek SK, Jan-Niklas M, Benjamin T, Lia A, Natascha D, Fabian K, et al. Tumor targeting *via* EPR: strategies to enhance patient responses. *Adv Drug Deliv Rev* 2018;**130**:17–38.
6. Maeda Hiroshi. Toward a full understanding of the EPR effect in primary and metastatic tumors as well as issues related to its heterogeneity. *Adv Drug Deliv Rev* 2015;**91**:3–6.
7. Upendra B, Sindhu D, Nagavendra K, Wahid K. Liposomal formulations in clinical use: an updated review. *Pharmaceutics* 2017;**9**:12.
8. Ragelle HS, Danhier F, Préat V, Langer R, Anderson DG. Nanoparticle-based drug delivery systems: a commercial and regulatory outlook as the field matures. *Expet Opin Drug Deliv* 2017;**14**:851–64.
9. Farjadian F, Ghasemi A, Gohari O, Roointan A, Karimi M, Hamblin MR. Nanopharmaceuticals and nanomedicines currently on the market: challenges and opportunities. *Nanomedicine* 2019;**14**:93–126.
10. Li C, Wang J, Wang Y, Gao H, Wei G, Huang Y, et al. Recent progress in drug delivery. *Acta Pharm Sin B* 2019;**9**:1145–62.
11. He H, Lu Y, Qi J, Zhu Q, Chen Z, Wu W. Adapting liposomes for oral drug delivery. *Acta Pharm Sin B* 2019;**9**:36–48.

12. Düzgüneş N, Gregoriadis G. Introduction: the origins of liposomes: Alec Bangham at Babraham. *Methods Enzymol* 2005;**391**:1−3.
13. Patil Yogita P, Jadhav Sameer. Novel methods for liposome preparation. *Chem Phys Lipids* 2014;**177**:8−18.
14. Wang Y, Grainger DW. Lyophilized liposome-based parenteral drug development: reviewing complex product design strategies and current regulatory environments. *Adv Drug Deliv Rev* 2019;**151**−**152**:56−71.
15. Sihem AO, Donald M, Robert S. Application of pharmacokinetic and pharmacodynamic analysis to the development of liposomal formulations for oncology. *Pharmaceutics* 2014;**6**:137−74.
16. Gubernator Jerzy. Active methods of drug loading into liposomes: recent strategies for stable drug entrapment and increased *in vivo* activity. *Expet Opin Drug Deliv* 2011;**8**:565−80.
17. Clerc S, Barenholz Y. Loading of amphipathic weak acids into liposomes in response to transmembrane calcium acetate gradients. *Biochim Biophys Acta* 1995;**1240**:257−65.
18. Barenholz Y. Doxil®—the first FDA-approved nano-drug: lessons learned. *J Contr Release* 2012;**160**:117−34.
19. Wehbe M, Chernov L, Chen K, Bally MB. PRCosomes: pretty reactive complexes formed in liposomes. *J Drug Target* 2016;**24**:1−26.
20. Tang WL, Tang WH, Szeitz A, Kulkarni J, Cullis P, Li SD. Systemic study of solvent-assisted active loading of gambogic acid into liposomes and its formulation optimization for improved delivery. *Biomaterials* 2018;**166**:13−26.
21. Sur S, Fries AC, Kinzler KW, Zhou S, Vogelstein B. Remote loading of preencapsulated drugs into stealth liposomes. *Proc Natl Acad Sci U S A* 2014;**111**:2283−8.
22. Zhigaltsev IV, Winters G, Srinivasulu M, Crawford J, Wong M, Amankwa L, et al. Development of a weak-base docetaxel derivative that can be loaded into lipid nanoparticles. *J Contr Release* 2010;**144**:332−40.
23. May J, Undzys E, Roy A, Li SD. Synthesis of a gemcitabine pro-drug for remote loading into liposomes and improved therapeutic effect. *Bioconjugate Chem* 2016;**27**:226−37.
24. Yang Wenqian, Yang Zimeng, Fu Jingru, Guo Mengran, Sun Bingjun, Wei Wei, et al. The influence of trapping agents on the antitumor efficacy of irinotecan liposomes: head-to-head comparison of ammonium sulfate, sulfobutylether-$\beta$-cyclodextrin and sucrose octasulfate. *Biomater Sci* 2018;**7**:419−28.
25. Hoshyar N, Gray S, Han H, Bao G. The effect of nanoparticle size on *in vivo* pharmacokinetics and cellular interaction. *Nanomedicine* 2016;**11**:673−92.
26. Cheng Yang, Zou Tao, Dai Min, He Xiaoyan, Peng Na, Wu Kui, et al. Doxorubicin loaded tumor-triggered targeting ammonium bicarbonate liposomes for tumor-specific drug delivery. *Colloids Surf B Biointerfaces* 2019;**178**:263−8.
27. Raghunand N, Mahoney BP, Gillies RJ. Tumor acidity, ion trapping and chemotherapeutics. II. pH-Dependent partition coefficients predict importance of ion trapping on pharmacokinetics of weakly basic chemotherapeutic agents. *Biochem Pharmacol* 2003;**66**:1219−29.
28. Abumanhal-Masarweh H, Koren L, Zinger A, Yaari Z, Krinsky N, Kaneti G, et al. Sodium bicarbonate nanoparticles modulate the tumor pH and enhance the cellular uptake of doxorubicin. *J Contr Release* 2019;**296**:1−13.
29. Wang Z, Chi D, Wu X, Wang Y, Lin X, Xu Z, et al. Tyrosine modified irinotecan-loaded liposomes capable of simultaneously targeting LAT1 and $ATB^{0,+}$ for efficient tumor therapy. *J Contr Release* 2019;**316**:22−33.
30. Yan J, Allen S, Vijayan D, Li XY, Harjunpää H, Takeda K, et al. Experimental lung metastases in mice are more effectively inhibited by blockade of IL23R than IL23. *Cancer Immunol Res* 2018;**6**:978.
31. Seidi Farzad, Jenjob Ratchapol, Crespy Daniel. Designing smart polymer conjugates for controlled release of payloads. *Chem Rev* 2018;**118**:3965−4036.
32. Mills E, O'Neill LAJ. Succinate: a metabolic signal in inflammation. *Trends Cell Biol* 2014;**24**:313−20.
33. Papatriantafyllou Maria. A pro-inflammatory role for succinate. *Nat Rev Immunol* 2013;**13**:305.
34. Zucker D, Marcus D, Barenholz Y, Goldblum A. Liposome drugs' loading efficiency: a working model based on loading conditions and drug's physicochemical properties. *J Contr Release* 2009;**139**:73−80.
35. Johnston MJ, Semple SC, Klimuk SK, Edwards K, Eisenhardt ML, Leng EC, et al. Therapeutically optimized rates of drug release can be achieved by varying the drug-to-lipid ratio in liposomal vincristine formulations. *Biochim Biophys Acta* 2006;**1758**:55−64.
36. Johnston MJ, Edwards K, Karlsson G, Cullis PR. Influence of drug-to-lipid ratio on drug release properties and liposome integrity in liposomal doxorubicin formulations. *J Liposome Res* 2008;**18**:145−57.
37. Sun B, Straubinger RM, Lovell JF. Current taxane formulations and emerging cabazitaxel delivery systems. *Nano Res* 2018;**11**:5193−218.
38. Zhang YN, Poon W, Tavares AJ, Mcgilvray ID, Chan WCW. Nanoparticle−liver interactions: cellular uptake and hepatobiliary elimination. *J Contr Release* 2016;**240**:332−48.
39. Horowitz Todd S, Suls Jerry, Treviño Melissa. A call for a neuroscience approach to cancer-related cognitive impairment. *Trends Neurosci* 2018;**41**:493−6.
40. Matsos A, Johnston IN. Chemotherapy-induced cognitive impairments: a systematic review of the animal literature. *Neurosci Biobehav Rev* 2019;**102**:382−99.
41. Karavelioğlu E, Gönül Y, Aksit H, Boyaci MG, Rakip U. Cabazitaxel causes a dose-dependent central nervous system toxicity in rats. *J Neurol Sci* 2016;**360**:66−71.
42. Christie LA, Acharya MM, Parihar VK, Nguyen A, Martirosian V, Limoli CL. Impaired cognitive function and hippocampal neurogenesis following cancer chemotherapy. *Clin Canc Res* 2012;**18**:1954.
43. Kroon J, Metselaar JM, Storm G, van der Pluijm G. Liposomal nanomedicines in the treatment of prostate cancer. *Canc Treat Rev* 2014;**40**:578−84.
44. Lv Q, Yang X, Wang M, Yang J, Qin Z, Kan Q, et al. Mitochondria-targeted prostate cancer therapy using a near-infrared fluorescence dye−monoamine oxidase A inhibitor conjugate. *J Contr Release* 2018;**279**:234−42.
45. Quail DF, Joyce JA. Microenvironmental regulation of tumor progression and metastasis. *Nat Med* 2013;**19**:1423−37.